

Self-supervised learning for gravitational wave signal identification

Yu-Tong Wang^{1,2*}, Hao-Yang Liu^{3†}, and Yun-Song Piao^{1,2,3,4 ‡}

¹ *International Center for Theoretical Physics Asia-Pacific, Beijing/Hangzhou, China*

² *School of Fundamental Physics and Mathematical Sciences,*

Hangzhou Institute for Advanced Study, UCAS, Hangzhou 310024, China

³ *School of Physics Sciences, University of Chinese Academy of Sciences, Beijing 100049, China and*

⁴ *Institute of Theoretical Physics, Chinese Academy of Sciences, P.O. Box 2735, Beijing 100190, China*

The computational cost of searching for gravitational wave (GW) signals in low latency has always been a matter of concern. We present a self-supervised learning model applicable to the GW detection. Based on simulated massive black hole binary signals in synthetic Gaussian noise representative of space-based GW detectors Taiji and LISA sensitivity, and regarding their corresponding datasets as a GW twins in the contrastive learning method, we show that the self-supervised learning may be a highly computationally efficient method for GW signal identification.

PACS numbers:

I. INTRODUCTION

The field of gravitational wave (GW) detection has seen an explosion of compact binary coalescence signals over the past several years [1–6]. Recently, 93 GW events have been reported [7]. It is expected that over the coming years, more GW events, including binary black holes (BBH), binary neutron stars (BNS), as well as other exotic sources will be observed more frequently. As such, the need for more efficient search methods will be more important as the detectors improve in sensitivity.

It is well-known that identifying signal is achieved, in part, using a technique known as template-based matched filtering, which uses a bank [8–12] of template waveforms [13–16] spanning a large astrophysical parameter space. The corresponding waveform models that cover the inspiral, merger, and ringdown phases of a compact binary coalescence are based on combining post-Newtonian theory [17–19], the effective-one-body method [20], and numerical relativity simulations [21]. However, the algorithms used by the search pipelines to make detections are computationally expensive, since the large parameter space, as well as analysis of the high frequency components of the waveform, inevitably result in large computational cost.

Recently, the deep learning has been in popularity [22–26], which is a subset of machine learning. The advantage of deep learning is that the computationally intensive stage is pre-computed, so it is able to performing analyses rapidly. Its successful implementations include image processing [27, 28], medical diagnosis, in particular GW field, such as glitch classification [29–31] and signal identification [32–44].

However, the deep learning method currently used for searching for the GW signals is often limited to building

supervised learning models, which are indeed trained on scarcely labelled or simulated data and thus suffer from biases or small training sizes when applied to new or full datasets. Thus it is significant to consider the tailored deep learning models in a self-supervised, semi-supervised or unsupervised manner [45, 46].

In this paper, we report the construction of a self-supervised learning that can reproduce the searching for massive black hole binary (MBHB) GW signals. A contrastive learning method, the GW twins, which applies redundancy-reduction to self-supervised learning [47], is proposed. Based on simulated MBHB signals in synthetic Gaussian noise representative of space-based GW detectors Taiji [48] and LISA [49] sensitivity, we investigate whether the self-supervised learning can efficiently identify a signal present in the data, or the data contain only detector noise.

II. METHOD

A. Description of GW twins

In self-supervised learning for GW detection, our GW twins operates on a joint embedding of augmentation vectors, see Fig.1. In detail, it produces two augmentation vectors for all data of a batch h sampled from a dataset. In our case, we consider the batch of h as an injected GW waveform signal. The augmentation vectors are obtained with a distribution of data augmentations \mathcal{T} (the light blue area in Fig.1). Two batches of augmentation vectors d^A and d^B are fed to a deep network f_θ (covered by the light yellow area in Fig.1), producing batches of embeddings h^A and h^B , respectively.

In our GW twins design, the corresponding loss function \mathcal{L}_{GW} is

$$\mathcal{L}_{GW} = \underbrace{\sum_i (1 - C_{ii}^{GW})^2}_{\text{invariant part}} + \lambda \underbrace{\sum_i \sum_{j \neq i} (C_{ij}^{GW})^2}_{\text{redundancy reduction part}}, \quad (1)$$

*wangyutong@ucas.ac.cn

†liuhaoyang19@mails.ucas.ac.cn

‡yspiao@ucas.ac.cn

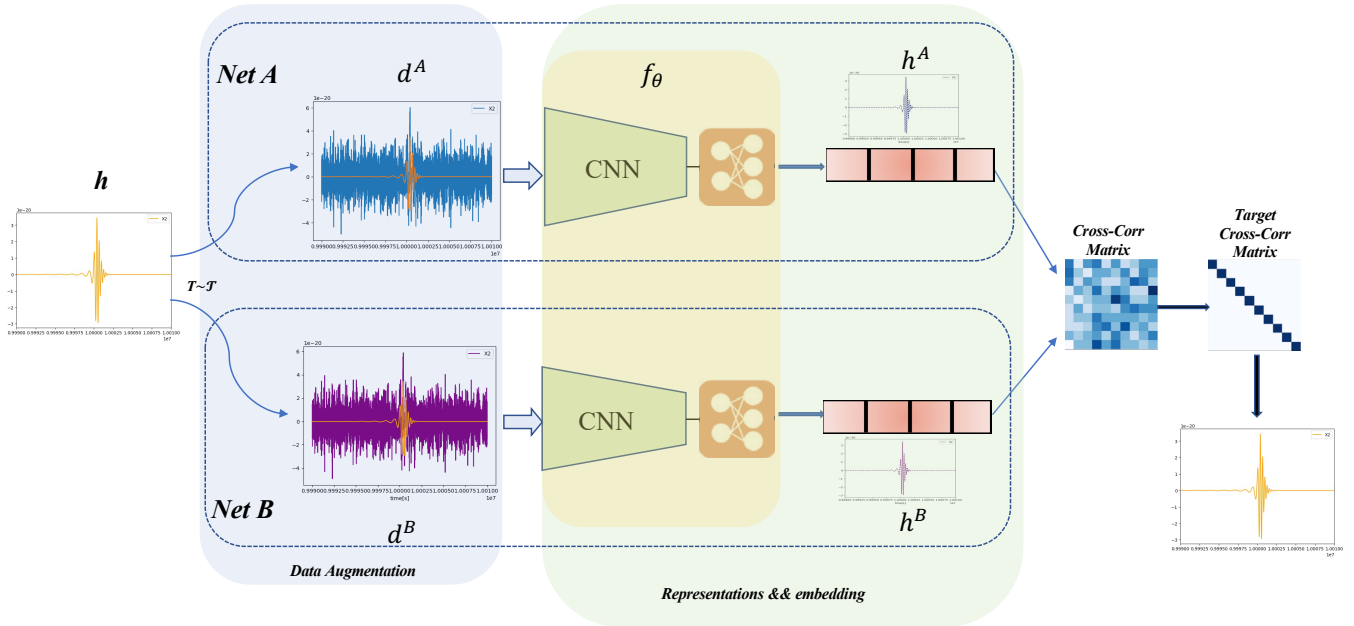


FIG. 1: The objective function of GW twins measures the cross-correlation matrix between the embeddings of two identical networks h^A and h^B (described as the extraction of GW signal by Net A and Net B) fed with augmentation versions of a batch of samples d^A and d^B (covered by the light blue area). Here, $d^A = h + n_L$ and $d^B = h + n_T$, and the cross-correlation matrix is made close to the identity. This causes the embedding vectors of distorted versions of a sample (blue and purple signal waveforms) to be similar, while minimizing the redundancy between the components of the embedding vectors.

where

$$C_{ij}^{GW} = \frac{\sum_b h_{b,i}^A h_{b,j}^B}{\sqrt{\sum_b (h_{b,i}^A)^2} \sqrt{\sum_b (h_{b,j}^B)^2}} \quad (2)$$

is the cross-correlation matrix computed between the outputs of two identical networks, with the values comprised between -1 (i.e. perfect anti-correlation) and 1 (i.e. perfect correlation), λ is a positive constant, b is batch samples, and i, j represent the vector dimension of the networks outputs

Here, the objective function (OF) is understood as an instantiation of the information bottleneck (IB) objective [50, 51]. It is easy to see that our OF has similarities with existing OFs for self-supervised learning, for example, the redundancy reduction part plays a role similar to the contrastive part in the INFONCE objective [52].

B. Implementation Details

It is often hard to find a large collection of correctly labelled data. This scarcity of labelled real data exists for GW events as well. One way to combat this shortage

is to train on simulated data and hope the trained model is useful for the real dataset as well. The success of such an approach is dependent on the quality of simulation. However, we will have rich raw data in GW detection, specially for space-based detectors, such as Taiji and LISA. Thus the application of self-supervised training can be particularly relevant for GW signal detection.

The basic idea of our GW twins design for self-supervised training is to have two dataset which see different versions of GW data and use the OF of GW twins to learn embeddings. In details, we can feed the data d^A from LISA into Net A and the data d^B from Taiji into Net B. In Fig.1, the blue strain and purple strain in the data augmentation waveform plottings which are covered by the light blue area correspond to the LISA noise data strain n_L and the Taiji noise data strain n_T , the orange waveform is the GW signal h . Since the noise in Taiji is different from LISA, we can imagine it as an augmented sample of the same underlying signal.

It is well-known that most self-supervised works focused on images, and so usually inputs are images and 2D CNN is used. However, for faster training we will use a 1D CNN model inspired by LISA mock data challenge. Moreover, we observed that adding a GRU layer and reducing the

original pooling size led to better results. We also removed the final fully connected layers since we require the models to produce embeddings. The bandpassed waveforms are fed as input to the model and we get embeddings of size 2048 as output.

In the original paper for calculating \mathcal{L}_{GW} in (1), they used LARS optimizer [53] but we found that AdamW with an initial learning rate of 10^{-4} also works, though LARS optimizer works better. Currently, we only using LISA mock data challenge and Taiji sensitivity curves generated noise as an additional augmentation.

The details about the contrastive learning work flow are list as follows:

Data augmentations The input data is first converted to produce the two augmentation vectors shown in Fig.1. The data augmentation pipeline includes: random cropping, resizing, horizontal flipping, color jittering, converting to grayscale, Gaussian blurring, and solarization. The cropping and resizing are always applied, while the last five are applied randomly, with some probability. This probability is different for the two augmentation vectors in the last two conversations (blurring and solarization). In this case we add the different space-based detectors noise into the input data, this data augmentation can be viewed as a color jittering. We use the same augmentation parameters as BYOL.

Architecture The encoder consists of a ResNet-50 network (without the final classification layer, 2048 output units) followed by a projector network. The projector network has three linear layers, each with 8192 output units. The first two layers of the projector are followed by a batch normalisation layer and rectified linear units. We call the output of encoder the “representations” and the output of projector the “embeddings”. The representations are used for downstream tasks and the embeddings are fed to \mathcal{L}_{GW} of our GW twins.

Optimization We follow the optimization protocol described in BYOL. The LARS optimizer is used, and we work for 1000 epochs with a batch size of 2048. We set the learning rate 0.2 for the weights and 0.0048 for the biases and batch normalization parameters. The learning rate warm-up period of 10 epochs is adopted, after which we lowered the learning rate by a factor of 1000 using a cosine decay schedule. The best results of λ in \mathcal{L}_{GW} is $\lambda = 5 \cdot 10^{-3}$.

III. SIMULATED SPACE-BASED GW DATASETS

A. Time-delay interferometry and noise budgets

Time-delay interferometry (TDI) will be employed for both LISA and Taiji to suppress the laser frequency noise and achieve targeting sensitivity. The principle of the TDI is to combine multiple time-shifted interferometric links and obtain an equivalent equal path for two interferometric laser beams. The GW response of TDI is combined by

the response of every single link. For a LISA-like with six laser links, three optimal TDI channels (A, E, T) could be constructed from three first-generation Michelson TDI configuration (X, Y, Z), see Refs. [54–61] for details about the TDI configuration.

By assuming laser frequency noise is sufficiently suppressed in TDI, the acceleration noise and optical path noise are considered to be the dominant noises for GW observation. The budgets of acceleration noise for LISA and Taiji are considered as same [49, 62],

$$S_{\text{acc}} = 9 \frac{\text{fm}^2/\text{s}^4}{\text{Hz}} \left[1 + \left(\frac{0.4 \text{ mHz}}{f} \right)^2 \right] \left[1 + \left(\frac{f}{8 \text{ mHz}} \right)^4 \right], \quad (3)$$

meanwhile, their optical path noise budgets are slightly different as

$$S_{\text{op,LISA}} = 100 \frac{\text{pm}^2}{\text{Hz}} \left[1 + \left(\frac{2 \text{ mHz}}{f} \right)^4 \right], \quad (4)$$

$$S_{\text{op,Taiji}} = 64 \frac{\text{pm}^2}{\text{Hz}} \left[1 + \left(\frac{2 \text{ mHz}}{f} \right)^4 \right]. \quad (5)$$

The power spectrum density (PSD) of noise which is presented in Fig. 2 is calculated by using the numerical method, see Refs. [57, 58] for detailed algorithm.

B. Data Curation

For simulated MBHB signals, we used SEOBNRv4_opt, which is a version of the SEOBNRv4 code [63] with significant optimizations, which can bring the signals for a high spin, high mass ratio MBHB system. We adopted the log-uniform distribution for the parameter M_{tot} from Ref. [64]. The sketch of waveform with the LDC dataset are shown in the time domain in Fig. 3 and the detailed parameters range is shown in Table I.

TABLE I: Summary of parameter setups in MBHB signal simulation.

Parameter	Lower bound	Upper bound
M_{tot}	$10^6 M_{\odot}$	$10^8 M_{\odot}$
q	0.1	10
s_1^z	-0.99	0.99
s_2^z	-0.99	0.99

Hereafter, we project the signal to space-based detector, and inject the projected signal to the noise with specific optimal SNR as

$$\text{SNR} = (s | s)^{-1/2}, \quad (6)$$

Here, s represents the signal, and $(h | s)$ is

$$(h | s) = 2 \int_{f_{\text{min}}}^{f_{\text{max}}} \frac{\tilde{h}^*(f)\tilde{s}(f) + \tilde{h}(f)\tilde{s}^*(f)}{S_n(f)} df, \quad (7)$$

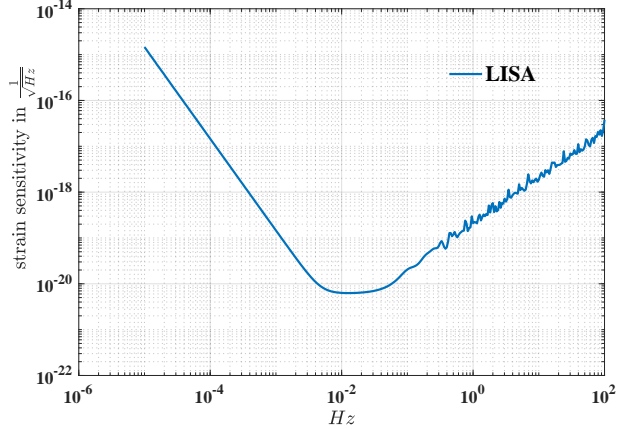
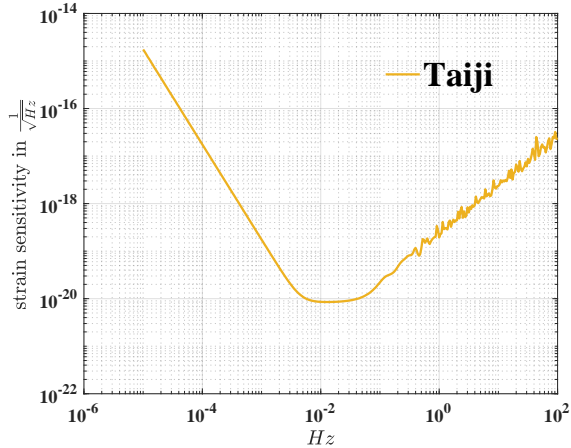


FIG. 2: The sensitivity curve of Taiji and LISA. The orange line is the sensitivity curve of Taiji and the blue line is the sensitivity curve of LISA.

where $f_{min} = 3 \times 10^{-5}$ Hz and $f_{max} = 0.05$ Hz, and $S_n(f)$ is the noise PSD. Here, following the setting of the LDC-2 dataset and Taiji configuration [65, 66], we set the SNR to 20. Then the data was whitened and normalized to $[-1, 1]$. During the whitening procedure, we applied the Tukey window with $\alpha = 1/8$.

IV. RESULTS

In our design for GW twins, Net A is responsible for the LISA embedding and Net B is for the Taiji embedding. The concatenation of all embeddings is used as input to the Fully connected (FC) layer. During the FC layer training, we freeze the backbone layer weights (Net A and B) and only train the FC layer on a subset of training dataset. To evaluate the ability of self-supervised learning, it is sufficient to train FC layer for 7-8 epochs, so we consider eight epoch,

Here, we list five targets for evaluating, AUC score, accuracy score, precision score, recall score and F1 score. The AUC stands for "Area under the ROC curve". An ROC curve is a graph showing the performance of a classification model at all classification thresholds. This curve plots two parameters, True Positive Rate (TPR) and False Positive Rate (FPR).

$$TPR = \frac{TP}{TP + FN}, \quad (8)$$

where TP stands for "True Positive" and FN stands for "False Negative",

$$FPR = \frac{FP}{FP + TN}, \quad (9)$$

where FP stands for "False Positive" and TN stands for "True Negative".

In Fig. 4, we can see the changing of AUC with the increasing epoch numbers. The maximum value of AUC is 0.85271 which corresponding the 7th epoches, while the value of AUC which corresponding 8th is slight small than the 7th's, it might be caused by the overfitting with the 1×1 convolution layer between the 7th and 8th, it also implied that 7 epoches is enough for our self-supervised learning and the ability of our model is good enough for the extraction of MBHB GW signal.

We also show the precision and recall. The Precision attempts to describe the proportion of actually correct positive identifications,

$$Precision = \frac{TP}{TP + FP}. \quad (10)$$

The Recall describes the proportion of identified correctly actual positives,

$$Recall = \frac{TP}{TP + FN}, \quad (11)$$

The Precision score are high values in the 7 epoches, which suggests that the self-supervised learning model can detect GW signal correctly.

In Fig. 6, we see that the levels of F1 score and accuracy are similar. It implies that the self-supervised learning model is hardly affected by the imbalance of data, which is the advantage of self-supervised learning model.

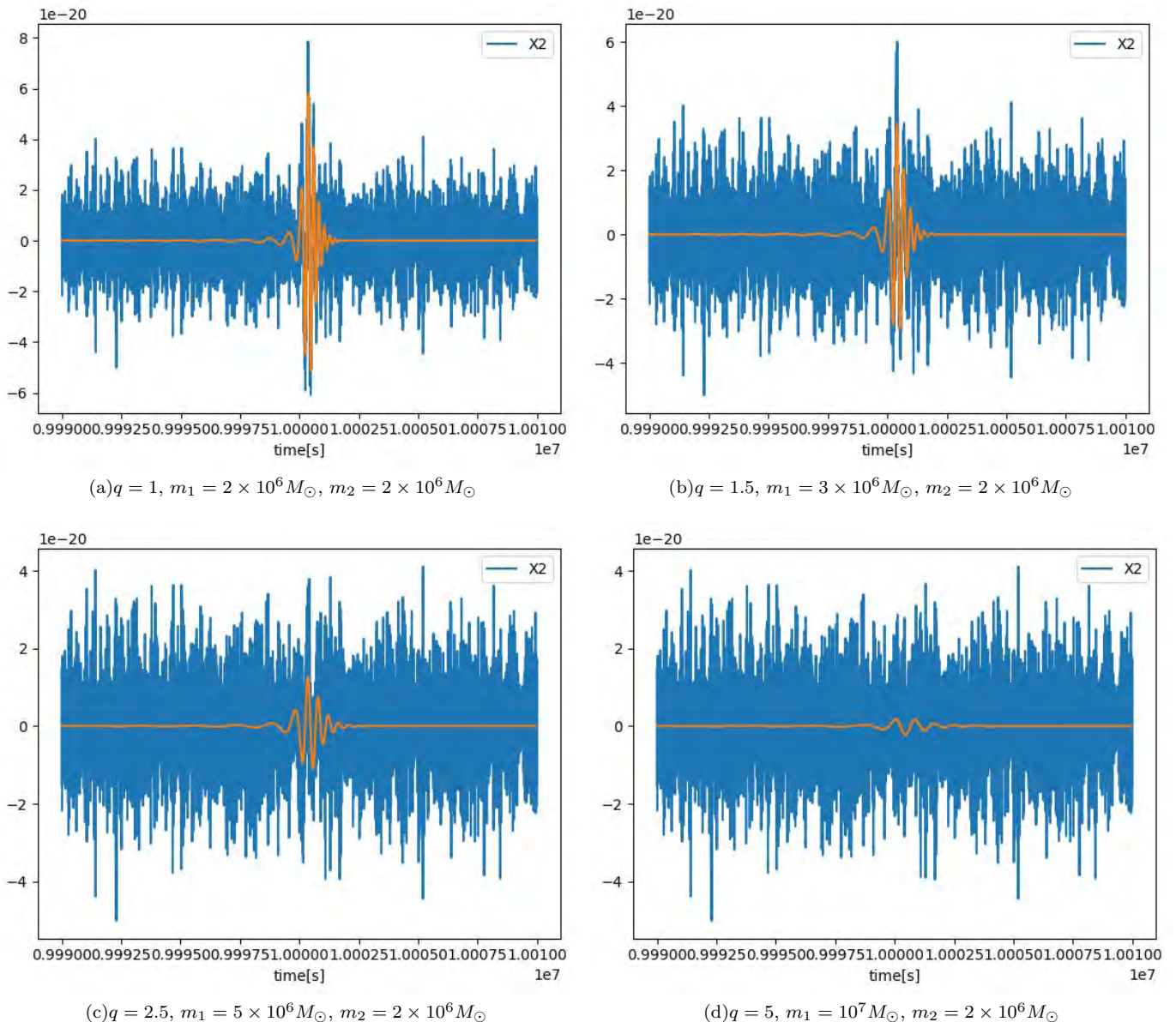


FIG. 3: Time domain representations of the TDI-X channel with different mass ratio $\frac{m_1}{m_2} = q$. The data from the LDC-2 dataset contain one MBHB signal presented by the orange line, the noise+signal data is presented by the blue line.

V. CONCLUSION

In this paper, we presented a self-supervised learning model applicable to the GW detection. Based on simulated massive black hole binary signals in synthetic Gaussian noise representative of space-based GW detectors Taiji and LISA sensitivity, we showed that the self-supervised learning is capable of implementing signal extraction, and can be a highly computationally efficient method for GW signal identification.

In corresponding contrastive learning method, we proposed the GW twins design operating on a joint embedding of augmentation vectors (here, Net A is for the LISA

embedding and Net B is for the Taiji embedding), which is conceptually simple, easy to implement. Benefits from such high-dimensional embeddings, it does not require large batches, nor does it require any asymmetric mechanisms like prediction networks, momentum encoders, non-differentiable operators or stop-gradients.

Though we have applied our method to the MBHB GW events, it also could be applied to other cases, such as binary white dwarf, extreme mass ratio inspirals. It might be also helpful to search for the GW echo signals, specially the unequal interval echoes [67–69]. The search for signals in GW data is mainly affected by non-Gaussian noise, actually, our method can be also applied to realistic non-Gaussian data, noting that the claim of matched-filtering

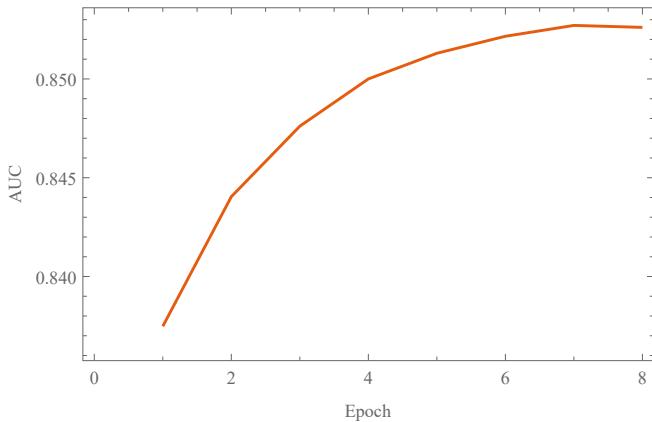


FIG. 4: AUC with respect to epoch.

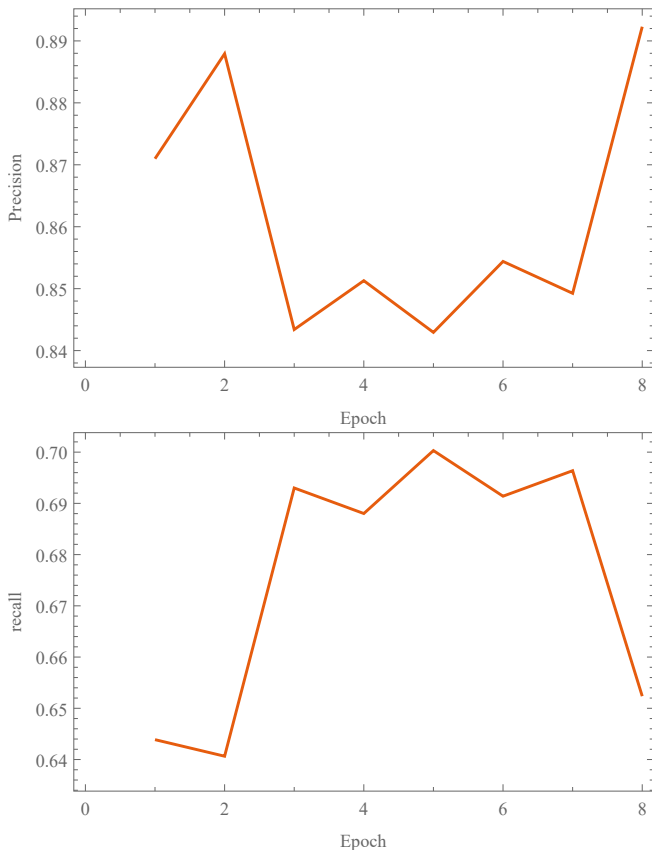


FIG. 5: Precision and Recall with respect to epoch.

optimality is applicable only in the Gaussian noise case. These interesting issues will be studied in the later works.

It also is worth mentioning that here we take the space-based GW detectors Taiji and LISA as a GW twins to present our method, however, self-supervised learning can also be applied in land-based GW detectors with high quality data well [70–72].

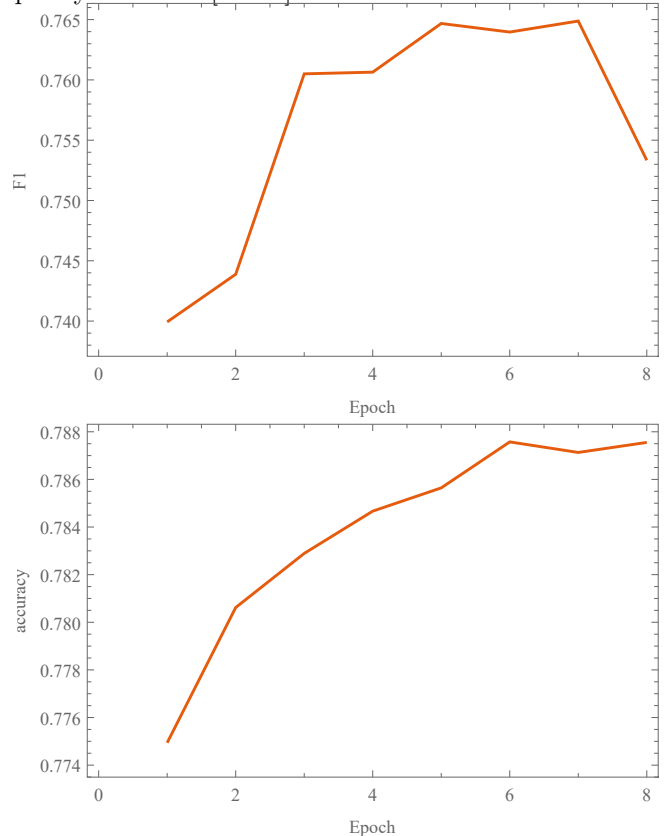


FIG. 6: F1 score and accuracy with respect to epoch.

VI. ACKNOWLEDGMENTS

YTW is supported by National Key Research and Development Program of China Grant No. 2021YFC2203004. YSP is supported by NSFC, No.12075246 and the Fundamental Research Funds for the Central Universities.

-
- [1] B. P. Abbott *et al.* [LIGO Scientific and Virgo], Phys. Rev. Lett. **116**, no.6, 061102 (2016) doi:10.1103/PhysRevLett.116.061102 [arXiv:1602.03837 [gr-qc]].
- [2] B. P. Abbott *et al.* [LIGO Scientific and Virgo], Phys. Rev. Lett. **116**, no.24, 241103 (2016) doi:10.1103/PhysRevLett.116.241103 [arXiv:1606.04855 [gr-qc]].

- [3] B. P. Abbott *et al.* [LIGO Scientific and VIRGO], Phys. Rev. Lett. **118**, no.22, 221101 (2017) [erratum: Phys. Rev. Lett. **121**, no.12, 129901 (2018)] doi:10.1103/PhysRevLett.118.221101 [arXiv:1706.01812 [gr-qc]].
- [4] B. P. Abbott *et al.* [LIGO Scientific and Virgo], Phys. Rev. Lett. **119**, no.16, 161101 (2017) doi:10.1103/PhysRevLett.119.161101 [arXiv:1710.05832]

- [gr-qc].
- [5] B. P. Abbott *et al.* [LIGO Scientific and Virgo], *Phys. Rev. X* **9**, no.3, 031040 (2019) doi:10.1103/PhysRevX.9.031040 [arXiv:1811.12907 [astro-ph.HE]].
- [6] R. Abbott *et al.* [LIGO Scientific and Virgo], *Phys. Rev. X* **11**, 021053 (2021) doi:10.1103/PhysRevX.11.021053 [arXiv:2010.14527 [gr-qc]].
- [7] R. Abbott *et al.* [LIGO Scientific, VIRGO and KAGRA], [arXiv:2111.03606 [gr-qc]].
- [8] D. A. Brown, I. Harry, A. Lundgren and A. H. Nitz, *Phys. Rev. D* **86**, 084017 (2012) doi:10.1103/PhysRevD.86.084017 [arXiv:1207.6406 [gr-qc]].
- [9] T. Dal Canton and I. W. Harry, [arXiv:1705.01845 [gr-qc]].
- [10] I. W. Harry, B. Allen and B. S. Sathyaprakash, *Phys. Rev. D* **80**, 104014 (2009) doi:10.1103/PhysRevD.80.104014 [arXiv:0908.2090 [gr-qc]].
- [11] T. Dal Canton, A. H. Nitz, A. P. Lundgren, A. B. Nielsen, D. A. Brown, T. Dent, I. W. Harry, B. Krishnan, A. J. Miller and K. Wette, *et al.* *Phys. Rev. D* **90**, no.8, 082004 (2014) doi:10.1103/PhysRevD.90.082004 [arXiv:1405.6731 [gr-qc]].
- [12] P. Ajith, N. Fotopoulos, S. Privitera, A. Neunzert and A. J. Weinstein, *Phys. Rev. D* **89**, no.8, 084041 (2014) doi:10.1103/PhysRevD.89.084041 [arXiv:1210.6666 [gr-qc]].
- [13] B. S. Sathyaprakash and S. V. Dhurandhar, *Phys. Rev. D* **44**, 3819-3834 (1991) doi:10.1103/PhysRevD.44.3819
- [14] A. Taracchini, A. Buonanno, Y. Pan, T. Hinderer, M. Boyle, D. A. Hemberger, L. E. Kidder, G. Lovelace, A. H. Mroué and H. P. Pfeiffer, *et al.* *Phys. Rev. D* **89**, no.6, 061502 (2014) doi:10.1103/PhysRevD.89.061502 [arXiv:1311.2544 [gr-qc]].
- [15] S. Privitera, S. R. P. Mohapatra, P. Ajith, K. Cannon, N. Fotopoulos, M. A. Frei, C. Hanna, A. J. Weinstein and J. T. Whelan, *Phys. Rev. D* **89**, no.2, 024003 (2014) doi:10.1103/PhysRevD.89.024003 [arXiv:1310.5633 [gr-qc]].
- [16] L. Blanchet, *Living Rev. Rel.* **17**, 2 (2014) doi:10.12942/lrr-2014-2 [arXiv:1310.1528 [gr-qc]].
- [17] K. G. Arun, A. Buonanno, G. Faye and E. Ochsner, *Phys. Rev. D* **79**, 104023 (2009) [erratum: *Phys. Rev. D* **84**, 049901 (2011)] doi:10.1103/PhysRevD.79.104023 [arXiv:0810.5336 [gr-qc]].
- [18] A. Buonanno, B. Iyer, E. Ochsner, Y. Pan and B. S. Sathyaprakash, *Phys. Rev. D* **80**, 084043 (2009) doi:10.1103/PhysRevD.80.084043 [arXiv:0907.0700 [gr-qc]].
- [19] C. K. Mishra, A. Kela, K. G. Arun and G. Faye, *Phys. Rev. D* **93**, no.8, 084054 (2016) doi:10.1103/PhysRevD.93.084054 [arXiv:1601.05588 [gr-qc]].
- [20] A. Buonanno and T. Damour, *Phys. Rev. D* **59**, 084006 (1999) doi:10.1103/PhysRevD.59.084006 [arXiv:gr-qc/9811091 [gr-qc]].
- [21] F. Pretorius, *Phys. Rev. Lett.* **95**, 121101 (2005) doi:10.1103/PhysRevLett.95.121101 [arXiv:gr-qc/0507014 [gr-qc]].
- [22] I. J. Goodfellow, J. Pouget-Abadie, M. Mirza, B. Xu, D. Warde-Farley, S. Ozair, A. Courville and Y. Bengio, [arXiv:1406.2661 [stat.ML]].
- [23] K. Simonyan and A. Zisserman, [arXiv:1409.1556 [cs.CV]].
- [24] Liang-Chieh Chen, George Papandreou, Iasonas Kokkinos, Kevin Murphy, Alan L. Yuille [arXiv:1412.7062 [cs.CV]].
- [25] Matthew D Zeiler, Rob Fergus [arXiv:1311.2901 [cs.CV]].
- [26] C. Szegedy, W. Liu, Y. Jia, P. Sermanet, S. Reed, D. Anguelov, D. Erhan, V. Vanhoucke and A. Rabinovich, [arXiv:1409.4842 [cs.CV]].
- [27] R. Zhang, P. Isola, A. A. Efros, [arXiv:1603.08511 [cs.CV]].
- [28] Andrej Karpathy, Li Fei-Fei [arXiv:1412.2306 [cs.CV]].
- [29] N. Mukund, S. Abraham, S. Kandhasamy, S. Mitra and N. S. Philip, *Phys. Rev. D* **95**, no.10, 104059 (2017) doi:10.1103/PhysRevD.95.104059 [arXiv:1609.07259 [astro-ph.IM]].
- [30] M. Zevin, S. Coughlin, S. Bahaadini, E. Besler, N. Rohani, S. Allen, M. Cabero, K. Crowston, A. Katsaggelos and S. Larson, *et al.* *Class. Quant. Grav.* **34**, no.6, 064003 (2017) doi:10.1088/1361-6382/aa5cea [arXiv:1611.04596 [gr-qc]].
- [31] D. George, H. Shen and E. A. Huerta, [arXiv:1706.07446 [gr-qc]].
- [32] D. George and E. A. Huerta, *Phys. Rev. D* **97**, no.4, 044039 (2018) doi:10.1103/PhysRevD.97.044039 [arXiv:1701.00008 [astro-ph.IM]].
- [33] W. Wei and E. A. Huerta, *Phys. Lett. B* **800**, 135081 (2020) doi:10.1016/j.physletb.2019.135081 [arXiv:1901.00869 [gr-qc]].
- [34] H. Xia, L. Shao, J. Zhao and Z. Cao, *Phys. Rev. D* **103**, no.2, 024040 (2021) doi:10.1103/PhysRevD.103.024040 [arXiv:2011.04418 [astro-ph.HE]].
- [35] Y. C. Lin and J. H. P. Wu, *Phys. Rev. D* **103**, no.6, 063034 (2021) doi:10.1103/PhysRevD.103.063034 [arXiv:2007.04176 [astro-ph.IM]].
- [36] C. H. Liao and F. L. Lin, *Phys. Rev. D* **103**, no.12, 124051 (2021) doi:10.1103/PhysRevD.103.124051 [arXiv:2101.06685 [astro-ph.IM]].
- [37] W. H. Ruan, H. Wang, C. Liu and Z. K. Guo, [arXiv:2111.14546 [astro-ph.IM]].
- [38] P. Bacon, A. Trovato and M. Bejger, [arXiv:2205.13513 [gr-qc]].
- [39] T. Zhao, R. Lyu, Z. Ren, H. Wang and Z. Cao, [arXiv:2207.07414 [gr-qc]].
- [40] M. B. Schäfer, O. Zelenka, A. H. Nitz, H. Wang, S. Wu, Z. K. Guo, Z. Cao, Z. Ren, P. Nousi and N. Stergioulas, *et al.* [arXiv:2209.11146 [astro-ph.IM]].
- [41] C. Murali and D. Lumley, [arXiv:2210.01718 [gr-qc]].
- [42] P. Nousi, A. E. Koloniari, N. Passalis, P. Iosif, N. Stergioulas and A. Tefas, [arXiv:2211.01520 [gr-qc]].
- [43] H. Shen, E. A. Huerta, E. O'Shea, P. Kumar and Z. Zhao, *Mach. Learn. Sci. Tech.* **3**, no.1, 015007 (2022) doi:10.1088/2632-2153/ac3843 [arXiv:1903.01998 [gr-qc]].
- [44] Z. Ren, H. Wang, Y. Zhou, Z. K. Guo and Z. Cao, [arXiv:2212.14283 [gr-qc]].
- [45] T. Chen, S. Kornblith, M. Norouzi, G. Hinton, [arXiv:2002.05709 [cs.LG]].
- [46] I. Misra, L. Maaten, [arXiv:1912.01991 [cs.CV]].
- [47] J. Zbontar, L. Jing, I. Misra, Y. LeCun, S. Deny, [arXiv:2103.03230 [cs.CV]].
- [48] W. R. Hu and Y. L. Wu, *Natl. Sci. Rev.* **4**, no.5, 685-686 (2017) doi:10.1093/nsr/nwx116
- [49] P. Amaro-Seoane *et al.* [LISA], [arXiv:1702.00786 [astro-ph.IM]].
- [50] N. Tishby, F. C. Pereira, W. Bialek [arXiv:physics/0004057].
- [51] N. Tishby, N. Zaslavsky, [arXiv:1503.02406 [cs.LG]].
- [52] A. van den Oord, Y. Z. Li, O. Vinyals, [arXiv:1807.03748 [cs.LG]].

- [53] Y. You, I. Gitman, B. Ginsburg, [arXiv:1708.03888 [cs.CV]].
- [54] M. Otto, G. Heinzel and K. Danzmann, *Class. Quant. Grav.* **29**, 205003 (2012) doi:10.1088/0264-9381/29/20/205003
- [55] M. Otto, doi:10.15488/8545
- [56] M. Tinto and O. Hartwig, *Phys. Rev. D* **98**, no.4, 042003 (2018) doi:10.1103/PhysRevD.98.042003 [arXiv:1807.02594 [gr-qc]].
- [57] G. Wang, W. T. Ni, W. B. Han and C. F. Qiao, *Phys. Rev. D* **103**, no.12, 122006 (2021) doi:10.1103/PhysRevD.103.122006 [arXiv:2010.15544 [gr-qc]].
- [58] G. Wang and W. T. Ni, [arXiv:2008.05812 [gr-qc]].
- [59] G. Wang and W. B. Han, *Phys. Rev. D* **103**, no.6, 064021 (2021) doi:10.1103/PhysRevD.103.064021 [arXiv:2101.01991 [gr-qc]].
- [60] T. A. Prince, M. Tinto, S. L. Larson and J. W. Armstrong, *Phys. Rev. D* **66**, 122002 (2002) doi:10.1103/PhysRevD.66.122002 [arXiv:gr-qc/0209039 [gr-qc]].
- [61] M. Vallisneri, J. Crowder and M. Tinto, *Class. Quant. Grav.* **25**, 065005 (2008) doi:10.1088/0264-9381/25/6/065005 [arXiv:0710.4369 [gr-qc]].
- [62] Y. Yang, W. B. Han, Q. Yun, P. Xu and Z. Luo, *Mon. Not. Roy. Astron. Soc.* **512**, no.4, 6217-6224 (2022) doi:10.1093/mnras/stac920 [arXiv:2205.00408 [gr-qc]].
- [63] A. Bohé, L. Shao, A. Taracchini, A. Buonanno, S. Babak, I. W. Harry, I. Hinder, S. Ossokine, M. Pürrer and V. Raymond, *et al.* *Phys. Rev. D* **95**, no.4, 044028 (2017) doi:10.1103/PhysRevD.95.044028 [arXiv:1611.03703 [gr-qc]].
- [64] M. L. Katz, *Phys. Rev. D* **105**, no.4, 044055 (2022) doi:10.1103/PhysRevD.105.044055 [arXiv:2111.01064 [gr-qc]].
- [65] W. H. Ruan, Z. K. Guo, R. G. Cai and Y. Z. Zhang, *Int. J. Mod. Phys. A* **35**, no.17, 2050075 (2020) doi:10.1142/S0217751X2050075X [arXiv:1807.09495 [gr-qc]].
- [66] W. H. Ruan, C. Liu, Z. K. Guo, Y. L. Wu and R. G. Cai, *Nature Astron.* **4**, 108-109 (2020) doi:10.1038/s41550-019-1008-4 [arXiv:2002.03603 [gr-qc]].
- [67] Y. T. Wang, Z. P. Li, J. Zhang, S. Y. Zhou and Y. S. Piao, *Eur. Phys. J. C* **78** (2018) no.6, 482 doi:10.1140/epjc/s10052-018-5974-y [arXiv:1802.02003 [gr-qc]].
- [68] Y. T. Wang, J. Zhang and Y. S. Piao, *Phys. Lett. B* **795** (2019), 314-318 doi:10.1016/j.physletb.2019.06.036 [arXiv:1810.04885 [gr-qc]].
- [69] Z. P. Li and Y. S. Piao, *Phys. Rev. D* **100** (2019) no.4, 044023 doi:10.1103/PhysRevD.100.044023 [arXiv:1904.05652 [gr-qc]].
- [70] D. Davis *et al.* [LIGO], *Class. Quant. Grav.* **38**, no.13, 135014 (2021) doi:10.1088/1361-6382/abfd85 [arXiv:2101.11673 [astro-ph.IM]].
- [71] F. Acernese *et al.* [Virgo], [arXiv:2205.01555 [gr-qc]].
- [72] F. Acernese *et al.* [Virgo], [arXiv:2210.15633 [gr-qc]].